Nucleic Acids Research, 1999, Vol. 27, No. 4 **1145–1151**

The geometry of a synaptic intermediate in a pathway of bacteriophage λ site-specific recombination

Geoffrey Cassell, Robert Moision[1], Ely Rabani[2] and Anca Segall*

Department of Biology and Molecular Biology Institute, San Diego State University, 5500 Campanile Drive, San Diego, CA 92182-4614, USA, [1]Department of Chemistry, San Diego State University, San Diego, CA 92182, USA and [2]Department of Biology, University of California at San Diego, San Diego, CA 92093, USA

Received September 22, 1998; Revised December 4, 1998; Accepted December 15, 1998

ABSTRACT

Bacteriophage λ uses site-specific recombination to move its DNA into and out of the *Escherichia coli* genome. The recombination event is mediated by the phage-encoded integrase (Int) at short DNA sequences known as attachment (*att*) sites. Int catalyzes recombination via at least four distinct pathways, distinguishable by their requirements for accessory proteins and by the sequence of their substrates. The simplest recombination reaction catalyzed by Int does not require any accessory proteins and takes place between two *attL* sites. This reaction proceeds through an intermediate known as the straight-L bimolecular complex (SL-BMC), a stable complex which contains two *attL* sites synapsed by Int. We have investigated the orientation of the two substrates in the SL-BMC with respect to each other using two independent direct methods, a ligation assay and visualization by atomic force microscopy (AFM). Both show that the two DNA substrates in the complex are arranged in a tetrahedral or nearly square planar alignment skewed towards parallel. The DNA molecules in the complex are bent.

INTRODUCTION

Site-specific recombination is a common event in nature. Recombinases control gene expression and plasmid copy number, resolve replication and transposition intermediates, increase genetic diversity and mediate joining and separation of viral and host genomes. All of these reactions must be both specific and efficient in order to regenerate viable chromosomes. These attributes depend in large part on how recombinases recognize and juxtapose their substrates in synaptic complexes, but very little is known about this stage of recombination.

The integrase family of recombinases has no inherent restrictions for the orientation of substrates. Bacteriophage λ's integrase (Int) protein recombines all pairs of sites regardless of their orientation with respect to each other, as do its relatives, the bacteriophage P1 Cre protein and the yeast Flp protein (1). The Int protein catalyzes recombination between pairs of substrates known as *att* sites through four different pathways (*attP* and *attB* in integration; *attL* and *attR* in excision; reviewed in 1,2) and two distinct reactions between pairs of *attL* sites (3–6; the sites are shown in Fig. 1A). The simplest of the *attL* × *attL* reactions, the straight-L pathway, requires only Int, is inhibited by IHF and is inefficient as compared with the other three pathways (only 5–10% of substrates are converted to products) (4,6). In contrast, the bent-L pathway requires both Int and IHF and is as efficient as integration or excision (6). Both L × L pathways have been detected *in vivo* as well as *in vitro* (4,6).

The straight-L pathway proceeds through a stable synaptic intermediate, named the straight-L bimolecular complex (SL-BMC), which consists of two *attL* sites held together by Int (IHF interferes with formation of the complex). In order to support formation of the SL-BMC, each of the *attL* sites must possess both core-type and arm-type binding sites for the Int protein (Fig. 1A) and footprinting experiments showed that both core sites and all three arm sites of each DNA substrate are occupied in the complex (5). To accomodate this data, we proposed that at least some of the Int protomers form bridges between the arm site of one *attL* substrate and the core site of the second substrate. The geometric arrangement of sites in the complex must affect both its assembly as well as subsequent steps in the pathway leading to formation of products.

With one exception, no direct information is available about the geometry of substrates with respect to each other for any tyrosine recombinase (results of topological experiments cannot be extrapolated to predict the geometry of recombination intermediates; 7). Kim and Landy (8) proposed anti-parallel synapsis for excision. Sadowski and colleagues (9) have studied glutaraldehyde-trapped synaptic complexes assembled by Flp, but their experiments could not determine the alignment of substrates within the complexes. In certain circumstances, Flp treats its substrates as symmetrical and synapses them in either orientation (9). Experiments with synthetic Holliday junctions in several systems support a square planar geometry for the Holliday junction (with DNA ends equidistant from each other) and have been interpreted as suggesting anti-parallel alignment of DNA molecules (10–12). The co-crystal of the bacteriophage P1 Cre protein with a Holliday junction showed that the two sites of DNA

*To whom correspondence should be addressed. Tel: +1 619 594 4490; Fax: +1 619 594 5676; Email: asegall@sunstroke.sdsu.edu

The authors wish it to be known that, in their opinion, the first two authors should be regarded as joint First Authors

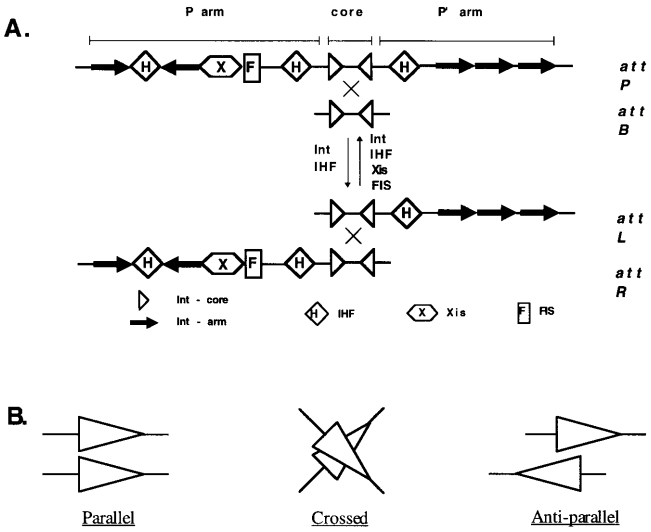

Figure 1. (**A**) Diagram of the *att* sites and the integration and excision reactions. Strand exchange occurs near each of the two Int core binding sites. The 0 coordinate of the *att* sites lies between the core sites. During straight-L recombination, the IHF site is not occupied (IHF inhibits straight-L recombination). (**B**) Models for the alignment of two *attL* sites in the SL-BMC. The *attL* sequence is depicted as an arrowhead. Any number of intermediate arrangements between the parallel, crossed and anti-parallel configurations are possible.

cleavage in the Holliday junction were diametrically opposed to each other in the structure, implying that the two DNA molecules are arranged in an anti-parallel orientation (13,14). A major difference among Int family enzymes involves the complexity of their recombination target sites and is reflected in the structure of the cognate recombinases. Int has an additional DNA binding domain not present in Cre, Flp or the Xer proteins, to accomodate the differences in target sequences (reviewed in 15,16). The stable SL-BMC intermediate presented an ideal opportunity to directly address the geometry of a synaptic complex at a stage that precedes the Holliday junction in an Int-mediated recombination pathway, in order to gain insight into how Int aligns its recombination substrates.

In order to define the orientation of the substrates with respect to each other, the polarity of the substrates must first be defined. Several elements within an *attL* molecule could lend polarity to the sequence; the main candidates are the relative position of Int core and arm binding sites and the 7 bp directional spacer, known as the overlap, between the two core binding sites (Fig. 1A). Formation of the SL-BMC, unlike recombination, does not depend on the identity of the overlap or on homology between overlap sequences on the two partner substrates (5). Therefore, the overlap does not contribute substantially to the polarity of the *attL* site in the complex. As stated above, efficient SL-BMC formation requires the presence on each partner substrate of both Int core and arm sites (5). Thus, their relative position may be an important element in determining site polarity.

An infinite number of possible alignments of the two sites exists in three-dimensional space, ranging from a strictly parallel arrangement to a symmetrically crossed (tetrahedral or square planar) arrangement, in which the four ends of the two DNA substrates are equidistant from each other, to a strictly anti-parallel arrangement (Fig 1B). We have examined the alignment of the *attL* substrates within the SL-BMC using both a ligation assay and visualization by atomic force microscopy (AFM). While these assays cannot make fine distinctions between closely related alignments, their results have shown that Int aligns the substrates in the SL-BMC in a nearly tetrahedral or square planar orientation which is skewed towards the parallel orientation. This resembles the arrangement of DNA molecules in the Cre–*lox* site co-crystal, but in that case the DNA molecules were arranged anti-parallel to each other. These two arangements may either reflect complexes at different stages during recombination or may reflect real differences between the Int and Cre enzymes.

MATERIALS AND METHODS

DNA substrates for the ligation assay

DNA fragments of four different sizes (130, 179, 224 and 230 bp) containing the *attL* sequence were generated by PCR using plasmid pHN872 as the template (17) and appropriate primers. The two shorter *attL* sites were designed with *Eag*I sites at either end of the fragment while the two longer *attL* sites were designed with *Eco*RI sites at either end. The PCR products were digested with *Eag*I or *Eco*RI (New England Biolabs) and gel purified using PAGE. Each fragment was radiolabeled in reactions containing 100 nM DNA, 25 µCi [γ-^{32}P]ATP (NEN) and 10 U T4 polynucleotide kinase (NEB) and diluted to a final concentration of 20 nM.

DNA substrates for atomic force microscopy

A 1050 and a 960 bp fragment containing the *attL* site were synthesized by PCR using pHN872 as template. The longer length improves the deposition of the DNA on mica. The ends of the fragments are asymmetrically disposed with respect to the *attL* sequence in order to distinguish the two possible alignments of the sites in the complex. The longer DNA molecule has 800 bp to the left of the 0 coordinate in the *attL* sequence (for reference, –2 is the site of top strand cleavage) and 250 bp to the right, while the shorter molecule has 610 bp to the left and 350 bp to the right of the 0 coordinate of *attL*.

Ligation assay

SL-BMCs were assembled in a 5 µl volume containing 0.65–1.4 nM labeled DNA, 18.3 nM Int or buffer, 13 mM Tris, 60 mM KCl, 0.26 mM EDTA, 1.5 µg tRNA, 15% glycerol and 1.9 µg BSA. Purified Int was the generous gift of H.Nash and C.Robertson (NIH). Reactions were incubated for 1 h on ice to inhibit recombination while allowing formation of the SL-BMC. In order to minimize ligation of DNA molecules from different SL-BMCs, reactions were diluted 6-fold with buffer containing the following constituents (final concentrations *after* dilution are given): 1.5 µg tRNA, 1.2 mM ATP, 12.8 mM $MgCl_2$ and 1.3 mM DTT. Lastly, 8 U T4 DNA ligase (NEB) were added. Ligation reactions were incubated at 16°C for 3 h. The products were separated on a 5% native polyacrylamide gel (29:1 acrylamide: bisacrylamide) in 0.5× TBE at 165 V. Two to four reactions were pooled in each gel lane and 10 reactions were assembled for each treatment. The wet gel was then imaged by autoradiography.

The bands corresponding to SL-BMCs and, in the case of reactions without Int, to a dimer of *attL* sites were excised from the gel and the slices were layered on a 5% polyacrylamide–SDS gel. Electrophoresis was carried out in Tris/Tricine/SDS buffer at 100 mA (18) and the wet gel was visualized by autoradiography. The ligation products were excised from the gel and the DNA was

eluted overnight in TE/0.1% SDS at 37°C. The eluted DNA was concentrated and digested with *Hin*fI (NEB). Digestion products were separated on a 5% polyacrylamide–SDS gel in Tris/Tricine/SDS buffer at 100 mA. The gel was dried and visualized using a Molecular Dynamics PhosphorImager.

Terminal deoxynucleotidyl-transferase (TdT) reactions were performed according to the manufacturer's instructions (Boehringer Mannheim) using 10 µCi [α-^{32}P]dGTP (NEN). Exonuclease V (ExoV) digestions were carried out in 25 mM Tris–HCl, pH 8, 1 mM DTT, 5 mM $MgCl_2$, 1 mM ATP and 45 nM ExoV for 2 h at 37°C, then stopped with SDS loading buffer. ExoV was the generous gift of S. Kowalczykowski. Proteinase K digestions were carried out in parallel ligation reactions to which SDS (0.25% final concentration) and proteinase K (0.25 mg/ml final concentration) were added; reactions were incubated for 1 h at 37°C and separated as above.

Atomic force microscopy

SL-BMCs were assembled in a 20 µl reaction containing 10 mM HEPES, pH 8, 2 mM $MgCl_2$, 60 mM KCl, 50 µg/ml tRNA, 8 nM *attL* site (1050 bp or a mixture of the 1050 and 960 bp molecules) and 70 nM Int. These conditions were optimized for AFM as well as for SL-BMC formation. Less than 1–2% recombination is obtained in this buffer system due to the presence of HEPES instead of Tris buffer and low [$MgCl_2$] instead of spermidine. However, SL-BMCs form to ~50% of the level formed in Tris buffer (data not shown). Reactions were incubated for 35–60 min at room temperature. Five microliters of the mixture were diluted with 5 µl of Millipore-purified water and immediately deposited onto freshly cleaved mica disks (New York Mica Co.). After 2 min, the mica was washed with 10–15 drops of Millipore-purified water and dried in a stream of compressed 1,1,1,2-tetrafluoroethane to remove excess liquid and unbound particles.

The samples were viewed using a Nanoscope II atomic force microscope (Digital Instruments) in contact mode, using narrow 200 µm long silicon nitride cantilevers with oxide-sharpened tips and a force constant of 0.06 N/m. Imaging force, calculated from the force curve using these cantilevers, was typically ~1 nN. Imaging was performed at a scan speed of 5–8 Hz, in a fluid cell filled with reagent alcohol (90% ethanol, 4.5% methanol and 4.9% isopropanol) to minimize the tip force on the sample. Imaging under isopropanol has been shown to give better resolution than imaging in air (19). (It is estimated that imaging forces in liquids are typically 10 times smaller than imaging forces in air, causing less distortion and preventing possible cutting of the DNA by the tip.) Images were then processed by flattening to remove background slope. Nanoscope images were imported into NIH Image software for length measurements.

RESULTS

Ligation assay

The two DNA molecules in the SL-BMC should be ligated together in a specific orientation if the complex is stable and if the ends of the two DNAs are favorably aligned. In the absence of Int, on the other hand, DNA molecules should be ligated via random collision. Different ligation products will result for each orientation of the *attL* sites within the SL-BMC if both ends of both DNA substrates are ligated, if only one end of each substrate is ligated to the other or if ligation does not occur (Fig. 2). Cutting the

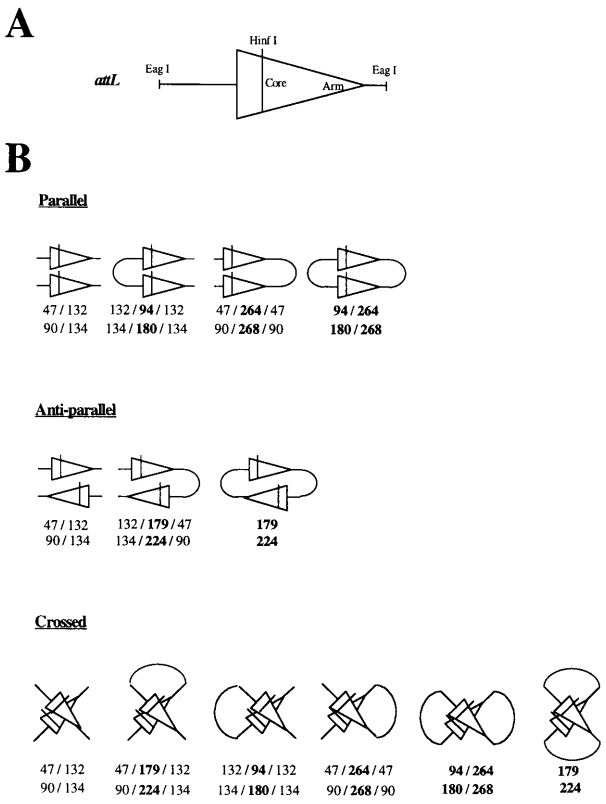

Figure 2. (**A**) Schematic representation of the ligation assay. The *attL* site is depicted as an arrowhead, with the *Hin*fI site off-center near the core. *Eag*I or *Eco*RI sites are present at both ends of the DNA fragment. (**B**) Ligation at the restriction sites of the fragments generates various dimeric product conformations depending on the initial alignment of the *att* sites in the SL-BMC. Subsequent digestion with *Hin*fI results in different fragments. The numbers below each diagram indicate the possible fragments obtained after digestion of that particular ligation product (the patterns for the 179 bp substrate are on top, the pattern for the 224 bp substrate below). Note that some patterns of fragments are shared between the crossed configuration and either the parallel or the anti-parallel configuration. However, the more symmetrical the crossed configuration is, the more possible fragments should be obtained after digestion.

ligation products at a different site (*Hin*fI) than the one used for ligation (*Eag*I or *Eco*RI) will generate fragments whose size depends on the initial alignment of the substrates. Four possible outcomes exist for the parallel alignment and three for the anti-parallel alignment. The crossed substrate configuration will yield a more complex mixture of products if all the ends are equally available to each other for ligation and depending on how skewed the alignment is towards the parallel or anti-parallel arrangements (Fig. 2, compare the 'crossed' arrangement with the 'parallel' and 'anti-parallel' arrangements). Each arrangement has certain diagnostic products, depending on the extent of ligation and the length of the substrate used in the reaction. The diagnostic fragments are shown in bold in Figure 2 (for simplicity, only fragment sizes for the 179 and 224 bp substrates are shown).

Figure 3A–D shows the results of a complete ligation experiment with the 179 bp substrate at different stages of the analysis. Briefly, ligase is added to reactions in which Int has assembled SL-BMCs or to *attL* molecules alone (Fig. 3A). Ligation products in the absence of Int should reflect random collision between *attL* sites. As expected, SL-BMC formation

depends on Int. Figure 3A also shows a control reaction in which ligase was absent. Some non-specific binding of ligase to the SL-BMCs appears to have caused retention of the complex in the well. Gel slices corresponding to the SL-BMCs and to *attL* ligated products obtained in the absence of Int were excised from the gel and electrophoresed through an SDS-containing gel (Fig. 3B). Ligation products were indeed obtained in all cases except where ligase was absent. At the concentration of ligase and DNA used, products with slower mobility were also obtained (Fig. 3B). In the case of the two shorter substrates, these products disappeared after proteinase K digestion (data not shown), showing that they were not simple ligation products, and were not analyzed here. Some of these are covalent complexes between Int and the *attL* site, since they are obtained in the absence of added ligase (Fig. 3B) (20; G.Cassell and A.Segall, manuscript in preparation).

The linearity of the ligation products was tested by sensitivity to digestion with ExoV, which requires a double-stranded end (21), and by the ability of the product to be labeled at the 3′-ends with [α-^{32}P]dGTP by TdT. Ligation products that were resistant to ExoV digestion and to TdT labeling were identified as circular and were found in the case of the two longer sites (data not shown). The circular products were analyzed and the results obtained agreed with the analysis of the linear dimer product (data not shown).

Ligation products that were sensitive to ExoV digestion and were labeled by TdT were deemed linear and their size was determined by comparison with molecular weight standards. Ligation products were eluted from the gel (each class was treated separately), concentrated and restricted with *Hin*fI, which cuts asymmetrically within the *attL* fragment. The restriction digests were electrophoresed on another SDS gel (Fig. 3C and D). As mentioned above, specific restriction fragments are diagnostic of different initial alignments. In the presence of Int and 179 bp substrate, fragments of 47, 132 and 264 bp were generated. This pattern is consistent with a parallel or nearly parallel alignment of the two *attL* molecules in the SL-BMC (refer to Fig. 2). Ligation evidently occurred at the end closest to the P′ arms of the *attL* sites (Fig. 1A), since the 94 bp fragment is absent. It is possible that Int facilitated ligation by bringing the two DNA molecules closest to each other at this end. The 132 and some of the 47 bp fragments presumably result from some unligated DNA that was carried along, despite gel isolation of the dimeric ligation product. The two ends of the fragment are differentially labeled, with the end closest to the arm sites labeled more than the end closest to the core sites (data not shown). This, as well as loss during ethanol precipitation, may account for some under-representation of the 47 bp fragment.

For ligation products obtained in the absence of Int, DNA fragments of 47, 94, 132, 179 and 264 bp are seen (Fig. 3C). The 179 bp fragment is diagnostic of anti-parallel alignment, while the 94 and 264 bp fragments are diagnostic of parallel alignment. The presence of fragments indicating both orientations is expected for ligation of sites in either orientation, as expected for DNA molecules brought together by random collision. In contrast, the presence of Int clearly biases the ligation products towards the parallel orientation.

The ligation assay was used with substrates of three other lengths in order to investigate further the arrangement of molecules within the complex. The 179 bp *attL* substrate was shortened at the core end by 24 bp and at the arm end by 25 bp, yielding a 130 bp substrate, to test whether proximity of the physical ends of the molecules to the Int binding sites stimulates ligation (if Int forces the ends closer to each other). The results obtained for the 130 bp substrate were the same as for the 179 bp substrate (Table 1): the arm ends were ligated, showing that Int bound at the arm sites does not occlude T4 DNA ligase, while the core ends remained unligated. Two related possibilities were tested: (i) that the core ends of the *attL* molecules were not long enough to be ligated; (ii) that the sticky ends could not be properly aligned for ligation due to their orientation along the helical axis of the DNA molecules. Therefore, substrates 224 and 230 bp in length were assayed in which the core ends were made 43 and 46 bp longer

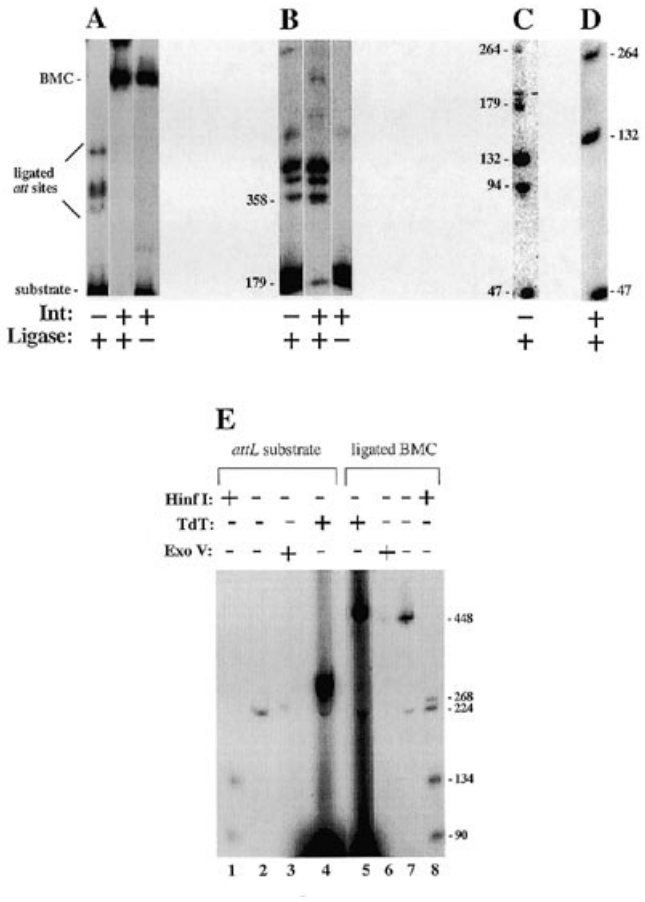

Figure 3. Ligation assay results using the 179 bp substrate (A–D) and the 224 bp substrate (E). (**A**) Electrophoretic mobility shift in the presence of ligase and/or Int. The SL-BMC bands and the ligated *att* products obtained in the absence of Int were excised from the gel and separated by SDS–PAGE. (**B**) SDS–PAGE separation of the ligation products. DNA corresponding to dimers of *attL* were eluted from the gel, concentrated and digested with *Hin*fI. (**C** and **D**) SDS–PAGE separation of the ligation products after restriction with *Hin*fI. The dimeric ligation products were excised from the gel, eluted and digested with *Hin*fI. The presence of both 94 and 264 bp fragments indicates both parallel and anti-parallel ligation in the absence of Int. The 264 bp fragment indicates parallel alignment of *attL* sites in the presence of Int. (**E**) Analysis of the 224 bp substrate products in the absence and presence of ligase. Lanes 2 and 7 represent the substrate control and the ligated product, respectively. Lanes 3 and 6 represent ExoV-treated substrate and ligated product, respectively. Lanes 4 and 5 represent TdT-treated substrate and ligation product, respectively. Lanes 1 and 8 represent *Hin*fI-treated substrate and ligated product, respectively. Experimental details are described in Materials and Methods.

than in the 179 bp molecule and the arm ends were lengthened by 2 and 5 bp, respectively (since ligation at the arm ends had already been seen, lengthening these ends significantly did not appear necessary). When each of these longer molecules was used to assemble SL-BMCs and subjected to ligation, we found that the two arm ends still ligated to each other, but also that an arm end ligated to a core end (Fig. 3E, Table 1 and data not shown). No linear ligation products were obtained in which the two core ends were ligated to each other. However, we obtained circular products for both of the two longer substrates, which contained *att* sites aligned either in the parallel or in the anti-parallel orientation (data summarized in Table 1). Thus ligation at the core ends does occur but is more difficult than ligation at the arm ends, since all molecules ligated at the core ends are also ligated at the arm ends. The data obtained with the 224 and 230 bp fragments led us to modify our earlier conclusion: the ends of the *attL* site are arranged both in a parallel and an anti-parallel alignment, i.e. a tetrahedral alignment, a square planar alignment or a mixture of parallel and anti-parallel alignments.

Table 1. Ligation products of SL-BMCs made with the four DNA substrates

Substrate	Core end to core end	Arm end to arm end	Core end to arm end
Linear ligation products			
130 bp (–45 to +85)	No	Yes	No
179 bp (–69 to +110)	No	Yes	No
224 bp (–112 to +112)	No	Yes	Yes
230 bp (–115 to +115)	No	Yes	Yes
Circular ligation products			
130 bp[a] (–45 to +85)	NA	NA	NA
179 bp[a] (–69 to +110)	NA	NA	NA
224 bp (–112 to +112)	Yes	Yes	Yes
230 bp (–115 to +115)	Yes	Yes	Yes

[a]Circular ligation products were not found for the 130 and 179 bp substrates.

Atomic force microscopy

The AFM images of SL-BMCs shown in Figure 4A–E clearly support a tetrahedral or square planar alignment that is skewed towards parallel of the two sites in the complex. Since the *attL* sequence is placed asymmetrically with respect to the ends of the DNA molecule, the orientation of the two molecules is easily observed. The DNA arms on either side of the Int globule were measured from the middle of the globule to the ends of the DNA: the long arm of each molecule had an average length of 293 ± 18 nm, the short arm averaged 55 ± 11 nm (24 complexes were measured). DNA imaged in propanol has a length of 3.4 ± 0.3 Å/bp, consistent with B-form DNA (22); we obtain ~3.3 Å/bp for the DNA in the SL-BMCs. The observed lengths eliminate the possibility of loops or large kinks in the complexes. Of roughly 60 SL-BMC images collected, three (5%) were anti-parallel (one is shown in Fig. 4F; Discussion). This is probably an over-estimate of the true proportion of anti-parallel complexes, since the total number of parallel SL-BMCs observed was higher than the actual number of images saved. Since anti-parallel complexes were relatively rare, all anti-parallel images were saved.

Because the two sites in the SL-BMC are equal in size, it is not possible to tell whether the two molecules cross each other or whether each bends at the location of the protein mass. To address this issue, we scanned complexes formed between the 1050 bp molecule and a shorter 960 bp molecule. The *attL* sequence is disposed on the two DNAs such that all four ends of the two molecules are identifiable. The resulting images indicate that the molecules do not cross within the complex, or if they cross, they wrap around each other once (Fig. 5). The observed images indicate that the molecules in the complex must be bent.

Images of single DNA molecules bound with Int also show the protein close to one end of the molecule, indicating that Int is binding specifically to the *attL* site (Fig. 4G and H). The lengths of DNA long and short segments in these complexes were 300 ± 12 and 54 ± 8 nm, respectively (average of 20 complexes). About 30% of the single DNA–Int complexes showed significant bends of the DNA coinciding with the location of Int. As expected, no SL-BMCs were observed in the absence of Int (data not shown).

The DNA width in the samples varied from 6 to 15 nm, which is comparable with previous results for contact mode imaging in isopropanol (19). The width of the DNA is dependent on the radius of curvature of the tip. The silicon nitride tips used have a nominal radius of curvature of 5–40 nm, but tip shape often changes while imaging a sample. The images clearly show the dependence on tip shape: the image in Figure 4A was scanned with a sharper tip than the image in Figure 4C. The background spots visible in the image are probably salt crystals and/or tRNA molecules that were not removed during sample preparation.

DISCUSSION

We have shown, using two independent direct assays, that the *attL* sites in a synaptic intermediate of recombination, the SL-BMC, are aligned in a tetrahedral or nearly square planar arrangement skewed towards parallel in most complexes. We believe that the complex cannot be completely planar since, given the arrangement of DNAs in the complex (Fig. 5), this would place the arm end and the core end of different molecules at the furthest distance from each other. This is very unlikely, since core–arm linear ligation products are obtained as readily as are arm–arm ligation products. In the absence of Int, DNA is ligated in both parallel and anti-parallel arrangements, as expected for the random collision of ends. Because the SL-BMC is a stable complex, no fixing agents such as protein–protein or protein–DNA crosslinkers were necessary and thus the architecture of the complex is as close to native as possible.

The two assays have many complementary features that strengthen our confidence in the results. (i) The ligation assay is performed in solution, while AFM requires deposition of the complexes onto a flat surface (surface deposition could possibly skew the conformation of the DNA). (ii) The ligation assay data is affected by the concentration of DNA in the reaction and some of the molecules ligated may be from different SL-BMCs, although we have no evidence of this. In contrast, AFM allows viewing of individual complexes. It is also possible that ligation is biased somewhat by the arrangement of Int molecules on the DNA molecule, i.e. ligation of molecules in one possible conformation would be inhibited because of improper juxtaposition of the DNA ends or interference by Int while ligation in the other conformation would be allowed. Neither of these are issues with AFM. (iii) AFM sample preparation may introduce a bias not

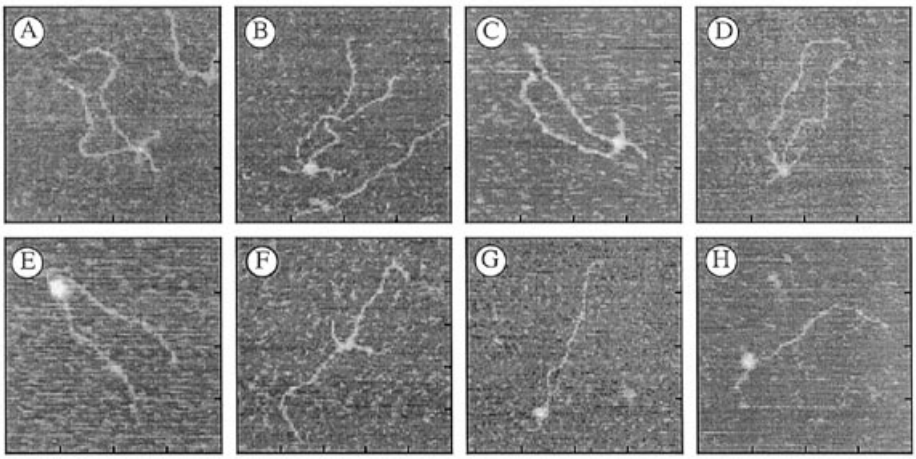

Figure 4. AFM images of SL-BMCs. In all cases, the DNA substrate is 1050 bp with the edge of the *attL* sequence ~160 bp from one end. Tick marks on the lower and right edges of each panel represent 100 nm intervals. (**A**–**D**) SL-BMCs showing parallel alignment of DNA strands (400 × 400 nm field). (**E**) Example of complex with a larger protein globule in the SL-BMCs (400 × 400 nm field). The size difference is likely due to non-specific binding of Int on DNA due to protein–protein interactions. (**F**) Anti-parallel SL-BMC (500 × 500 nm images). (**G**–**H**) Single DNA fragments with Int bound (400 × 400 nm image). Details of preparation in Materials and Methods.

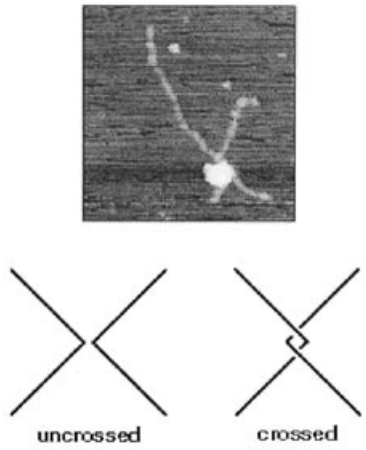

Figure 5. AFM image of SL-BMCs assembled with substrates of two different sizes, 1050 and 960 bp (300 × 300 nm image). Below the image are cartoons of two possible arrangements for the DNA molecules in the complex. The image is representative of nine complexes containing two different sizes of DNA molecules.

present during ligation; specifically, the steps of rinsing and removing excess liquid from the mica surface after deposition may have influenced the orientation of the complexes. This is unlikely because binding onto mica is fast (<2 min) and complex conformation is dependent on Int. In addition, single DNA molecules have Int bound at the same location with respect to the ends of the DNA molecule as the SL-BMCs. (iv) The ligation assay requires a lot of manipulations of the samples from the beginning to the end of the assay, while AFM methods require comparatively fewer manipulations. This points out the benefit of AFM analysis, which has already proven to be a powerful tool for investigating protein–DNA assemblies in their native conformation (reviewed in 23). To our knowledge, this is the first time AFM has been applied to intermediates of a recombination reaction.

During AFM imaging, a small proportion of anti-parallel complexes were observed. These could either be due to rare artefacts of sample preparation, occasional assembly of complexes with the DNAs in the opposite orientation or may represent a configuration at a later stage of the recombination reaction (although very little recombination takes place under the AFM conditions used; Materials and Methods). Since the sites appear to be arranged in a near tetrahedral alignment, relatively little movement of each pair of DNA ends would be required to give rise to an anti-parallel arrangement from the parallel arrangement. This agrees with the conclusions drawn from the Cre co-crystal data (13,14).

Preliminary results in an assay using tethered recombination targets indicate that the parallel orientation of the *att* site molecules at synapsis in the efficient bent-L pathway (6) favors recombination 2:1 over the anti-parallel orientation (W.Soward and A.Segall, unpublished results). This would suggest that Int aligns DNA molecules in a similar orientation for all the recombination pathways it catalyzes; we are currently testing this model for excision.

Int is not the only case that shows site alignment skewed towards parallel: unpublished electron microscopy data from S.Levene and colleagues shows that Flp protein also aligns its *frt* substrates in a parallel or near-parallel alignment (S.Levene, personal communication). Thus, two imaging methods and a ligation assay in two different recombination systems agree on the nature of the alignment, while crystallography points towards a nearly square planar alignment skewed towards anti-parallel. Electrophoretic analyses have been inferred to agree with the latter arrangement (11,12,24). Why do different methods give different answers? These results may point to the flexibility of the recombination machinery: at different stages of a recombination event, a near square planar or tetrahedral arragement may vary

between slightly parallel and slightly anti-parallel skews. During crystallization, it is possible that only one of these arrangements forms a crystal lattice, thereby selecting one form of the complex to the exclusion of the others. Imaging techniques, while imposing two-dimensional space on a three-dimensional complex, may nevertheless allow glimpses of more stages of the complex. Ligation can also be selective for the most easily trapped complex depending on the arrangement and length of the DNA arms. Nevertheless, ligation may sample more of the possible conformations present in solution than two-dimensional imaging or crystallographic methods. While parallel and anti-parallel arrangements suggest two extremes, the reality may be a series of dynamic complexes which progress through several conformations in the course of recombination.

In summary, using two direct assays, we have found that Int preferentially aligns *attL* sites in a synaptic recombination intermediate in a near tetrahedral or square planar arrangement which is skewed towards parallel. This alignment should place both strand exchange points near each other and thus should favor efficient recombination as seen for the integration, excision and bent-L recombination pathways. Thus, orientation of the substrates at synapsis does not explain the low efficiency of the straight-L reaction and the observed inefficiency must be due to a different factor. It is possible that this synaptic arrangement is in fact conformationally strained in the absence of a bending protein and that the alignment may not position the Int catalytic domain appropriately for one or both strand cleavage events. Experiments using sulfur-modified suicide substrates are being carried out to determine the step at which straight-L recombination is blocked.

Int has presumably evolved to perform efficiently in integration and excision; the straight-L reaction, in contrast, probably occurs rarely *in vivo* due to the presence of high levels of IHF. However, we believe that the stable SL-BMC has given us insight into a conserved property of Int and thus has proven useful in the study of the mechanism of λ site-specific recombination. The elucidation of the actual alignment of sites at synapsis should help guide the interpretation of data for both earlier and later steps of λ recombination.

ACKNOWLEDGEMENTS

We are extremely grateful to Doug Smith (UCSD) for lending us the Digital Instruments atomic force microscope and for encouragement throughout the project. We also thank Howard Nash, Kiyoshi Mizuuchi, Lea Jessop and Forest Rohwer for careful reading and incisive comments on the manuscript. This work was funded in part by NIGMS R01-52847 to A.M.S. and by a Sigma Xi grant from the San Diego chapter to R.M.

REFERENCES

1 Nash,H.A. (1996) In Neidhardt,F.C. *et al*. (eds), *Escherichia coli and Salmonella: Cellular and Molecular Biology.* ASM Press, Washington, DC, pp. 2363–2376.
2 Landy,A. (1989) *Annu. Rev. Biochem*., **58**, 913–949.
3 Echols,H. (1970) *J. Mol. Biol*., **47**, 575–583.
4 Kikuchi,A., Flamm,E. and Weisberg,R.A. (1985) *J. Virol*., **52**, 30–38.
5 Segall,A.M. and Nash,H.A. (1993) *EMBO J*., **12**, 4567–4576.
6 Segall,A.M. and Nash,H.A. (1996) *Genes Cells*, **1**, 453–463.
7 Sumners,D., Ernst,C., Spengler,S. and Cozarelli,N. (1995) *Q. Rev. Biophys*., **28**, 253–313.
8 Kim,S. and Landy,A. (1992) *Science*, **256**, 198–203.
9 Amin,A.A., Beatty,L.G. and Sadowski,P.D. (1990) *J. Mol. Biol*., **214**, 55–72.
10 Azaro,M. and Landy,A. (1997) *EMBO J*., **16**, 3744–3755.
11 Arciszewska,L., Grainge,I. and Sherratt,D. (1995) *EMBO J*., **14**, 2651–2660.
12 Lee,J., Voziyanov,Y., Pathania,S. and Jayaram,M. (1998) *Mol. Cell*, **1**, 483–493.
13 Guo,F., Gopaul,D.N. and Van Duyne,G.D. (1997) *Nature*, **389**, 40–46.
14 Gopaul,D.N., Guo,F. and Van Duyne,G.D. (1998) *EMBO J*., **17**, 4175–4187.
15 Esposito,D. and Scocca,J.J. (1997) *Nucleic Acids Res*., **25**, 3605–3614.
16 Nunes-Duby,S.E., Kwon,H.J., Tirumalai,R.S., Ellenberger,T. and Landy,A. (1998) *Nucleic Acids Res*., **26**, 391–406.
17 Nash,H.A. and Robertson,C.A. (1989) *EMBO J*., **8**, 3523–3533.
18 Schägger,H. and von Jagow,G. (1987) *Anal. Biochem*., **166**, 368–379.
19 Hansma,H.G., Vesenka,J., Siegerist,C., Kelderman,G., Morrett,H., Sinsheimer,R.L., Elings,V., Bustamante,C. and Hansma,P.K. (1992) *Science*, **256**, 1180–1184.
20 Pargellis,C.A., Nunes-Duby,S.E., Moitosos de Vargas,L. and Landy,A. (1988) *J. Biol. Chem*., **263**, 7678–7685.
21 Taylor,A.F. and Smith,G.R. (1985) *J. Mol Biol*., **185**, 431–443.
22 Hansma,H.G., Bezanilla,M., Zenhausern,F., Adrian,M. and Sinsheimer,R.L. (1993) *Nucleic Acids Res*., **21**, 505–512.
23 Bustamante,C. and Rivetti,C. (1996) *Annu. Rev. Biophys. Biomol. Struct*., **25**, 395–429.
24 Nunes-Duby,S., Azaro,M. and Landy,A. (1995) *Curr. Biol*., **5**, 139–148.